

## Research Article

# Synthetically Control of a Hybrid PV/FC/SC Power System for Stand-Alone Applications

<sup>1</sup>Guiting Xue, <sup>1</sup>Yan Zhang and <sup>2</sup>Dakang Zhu

<sup>1</sup>Shanghai Jiaotong University, Shanghai 200240, China

<sup>2</sup>Shanghai Municipal Electric Power Company, Shanghai 200122, China

**Abstract:** In this study, a simple and practical control scheme for power assignment and load-following of a Hybrid Power System (HPS) is proposed. The system consists of Photovoltaic (PV), Fuel Cell (FC), Super-Capacitor (SC), dc load, ac load and different kinds of converters. PV is chosen as a prior source, which normally operates in Maximum Power Point Tracking (MPPT) mode. In order to achieve 24 h power supply under various natural conditions, FC is used as a backup source to provide the power deficit between solar generation and load demand. Taking the slow FC system dynamics into account, FC power slope has been limited to protect FC from fuel starvation, whereas SC is chosen to satisfy the requirement of the sudden load and solar radiation changes. Besides, a V/f controller is designed to meet ac load demand, while keeping the voltage and frequency within an acceptable range. All the details of this study, including system structure, control diagrams and MATLAB simulation results, are presented.

**Keywords:** Fuel cell, hybrid power system, photovoltaic, super-capacitor, V/f control

## INTRODUCTION

Due to the ever-increasing energy consumption and rising public awareness of environmental protection, distributed generation technologies such as Photovoltaic (PV), Fuel Cell (FC), Wind Turbines (WT) and Micro Gas Turbines (MGT) are gaining interest (Jiayi *et al.*, 2008). Among them, solar power generation is one of the fastest-growing ones because solar radiation is clean, free and widely spread and less subjected to location constraints. Unfortunately, solar energy is an intermittent energy and the generated power is highly dependent on weather conditions (Ahmed *et al.*, 2008). In order to meet sustained load demand, PV system should be integrated with other renewable sources using hybrid topologies, that is known as Hybrid Power System (HPS) (Deshmukh and Deshmukh, 2008; Chicco and Mancarella, 2009).

The concept of HPS is not new. In the previous publications, lots of configurations and power management strategies for HPS have been reported. Hybrid PV-FC energy system was first proposed in (Rahman and Tam, 1988) it has shown that it is feasible to use FC in coordination with PV to meet variable load for either utility or stand-alone applications. An ac-linked hybrid PV-FC generation system with Maximum Power Point (MPP) controllers is presented in (Kyoungsoo and Rahman, 1998), which consists of two inverters, operating in parallel and outputs are tied to the utility grid via a multi-winding transformer. In

(Reddy and Agarwal, 2007), Reddy and Agarwal have been pointed out that the centralized dc-bus hybrid system with MPP trackers have some advantages against ac-bus category in terms of robustness, economics and easiness of applicable control. In (Caisheng and Nehrir, 2008), power management of stand-alone wind/photovoltaic/fuel cell energy system has been reported.

Because FC system has relatively slow response time, instantaneous power demand will cause fuel starvation, thus Super-Capacitor (SC) is necessary for FC to avoid fuel starvation and assure it a sufficient life-time (Thounthong *et al.*, 2009a). In Uzunoglu *et al.* (2009), special attention is given to model hybrid renewable energy system, but the fuel starvation problem is not considered. Energy management strategy of a hybrid PV/FC/SC energy system is proposed in Thounthong *et al.* (2011), the main contribution of the study is limiting the power slope of FC to avoid fuel starvation problems and improve performance. However, all the works mentioned above do not consider the reactive power demand and no controllers are utilized to maintain the voltage and frequency at Point of Common Coupling (PCC) within an acceptable level.

In this study, a synthetically control scheme of a stand-alone HPS consisting of PV/FC/SC is proposed. MPPT controller using fractional open circuit voltage is adopted by PV to exploit solar energy as much as possible; current slope limiter is employed by FC to

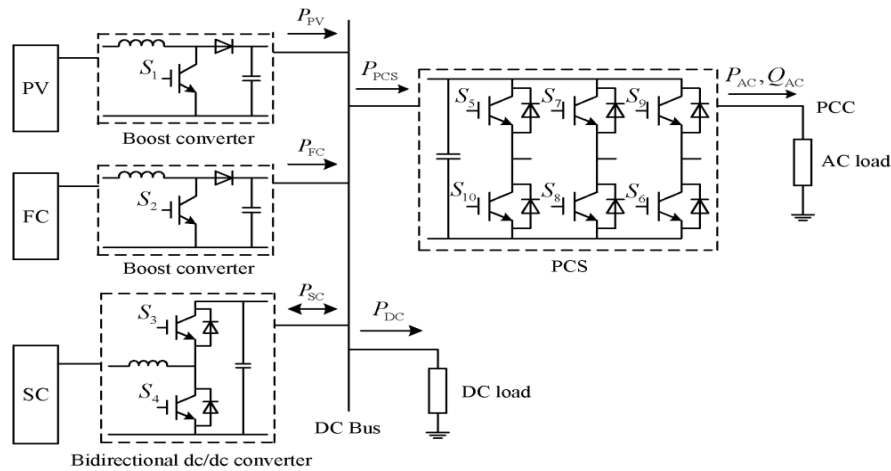


Fig. 1: The structure of HPS

prevent fuel starvation problems and improve its performance and lifetime; a controller with outer voltage loop plus inner current loop is applied to SC converter to compensate transient power and stabilize dc bus voltage. Furthermore, V/f controller is designed to satisfy both active and reactive load demand. The rest of this study is arranged as follows. Firstly, the structure and component model of HPS are presented; then, the control strategy for different converters is proposed; finally, simulation results are discussed and the conclusions are given.

**Structure and model:**

**Structure of HPS:** Four practical types of HPS have been used in the past:

- The centralized ac-bus
- The distributed ac-bus
- The centralized dc-bus
- The ac-dc hybrid structure

Because the third one has a lot of merits against the other three above categories (Reddy and Agarwal, 2007), so the centralized dc-coupled structure is adopted in this study, as shown in Fig. 1. In this topology, PV, FC and SC are connected to the common dc bus by boost converter, boost converter and bidirectional dc/dc converter, respectively. Then, the dc bus is connected to local ac load through the Power Conditioning System (PCS). PCS extracts energy from dc bus to provide active and reactive power for ac load.

**Component model:** As shown in Fig. 1, this HPS contains three kinds of micro sources: PV, FC and SC. The models described in Uzunoglu *et al.* (2009) are used in this study. For the details of model development, reader is referred to the aforementioned literature.

**Controller designs:**

**Controller design for PV:** PV has two operation states: Maximum Power Point Tracking (MPPT) and Constant Voltage (CV) generation. Normally, PV operates in MPPT mode to make the system efficient and dc bus voltage is regulated by SC converter; but the control scheme of PV must be switched from MPPT to CV control when SC has been fully charged, then the dc bus voltage is regulated by PV converter. The block diagram of PV control system is shown in Fig. 2. Where  $V_{DCRef}$  and  $V_{DC}$  are the dc-voltage reference and measured voltage, respectively;  $V_{SC}$  is SC terminal voltage and  $V_{SCMax}$  is SC maximum allowable voltage;  $V_{PV}$  and  $I_{PV}$  are the PV output voltage and output current, respectively.

Many MPPT algorithms have been proposed in the literatures, such as incremental conductance, fractional open circuit voltage and Perturbation and Observation (P and O) (Esram and Chapman, 2007). Each method has its own advantages and disadvantages. The fractional open circuit voltage method is used in this study because it is easy and cheap to implement. Equation (1) gives the near linear relationship between  $V_m$  and  $V_{oc}$  under varying irradiance and temperature levels:

$$V_m \approx k \cdot V_{oc} \tag{1}$$

where,

$V_m$  = The maximum power voltage

$V_{oc}$  = The open circuit voltage

$k$  = A constant of proportionality and has been reported to be between 0.71 and 0.78

Assuming continuous current mode for PV side boost converter, the following expressions are applicable:

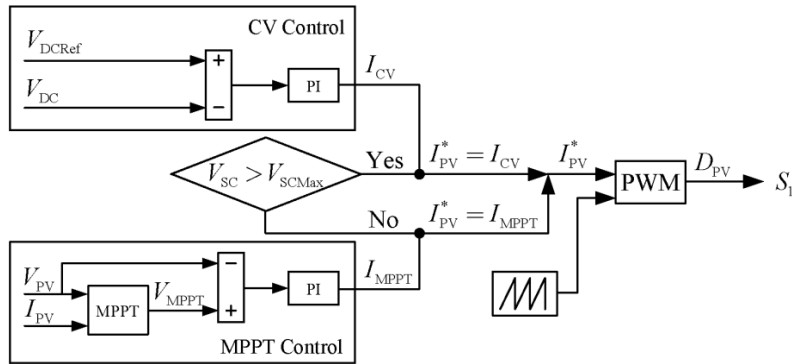


Fig. 2: Block diagram of PV control system

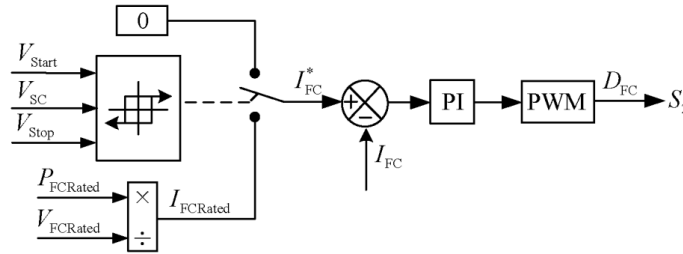


Fig. 3: Block diagram of the control scheme for FC

$$P_{PV} = I_{PV}V_{PV} \quad (2)$$

$$P_{PV} = I_{PV}V_{DC}(1 - D_{PV}) \quad (3)$$

where,

$D_{PV}$  = The duty cycle of boost converter and it should be governed to implement MPPT algorithm

**Controller design for FC:** FC plays a major role in balancing power, which has two working states: off and discharging? FC state depends only on SC terminal voltage. FC usually operates in standby state unless the terminal voltage of SC decreases below the start threshold  $V_{Start}$ . At this point, FC comes online, acting as constant power sources. Once SC terminal voltage exceeds the stop threshold  $V_{Stop}$ , FC will stop working. In order to keep high efficiency, FC should not be operated by a partial load condition, but operated by a start/stop control.

Figure 3 shows the block diagram of the implemented control scheme for FC. Conventional PI controller associated to a Pulse Width Modulation (PWM) generator is selected to directly control FC current  $I_{FC}$ . If  $V_{sc} < V_{start}$  FC current reference  $I_{FC}^*$  will be equal to  $I_{FCRated}$ . Once  $V_{sc} > V_{stop}$ ,  $I_{FC}^*$  becomes to be zero. Note that a “FC current slope limitation” is implemented to protect FC from fuel starvation. In

Fig. 3,  $P_{FCRated}$  and  $V_{FCRated}$  are the FC rated power and rated voltage, respectively.  $I_{FCRated}$  is the FC rated current?  $D_{FC}$  is the duty cycle of FC side boost converter. FC output power can be regulated through proper control of  $D_{FC}$ .

**Controller design for SC:** Due to quick charge/discharge time, good efficiency and long life cycle, SC is chosen to release or absorb transient power during startup or sudden load changes, thus keeping dc bus voltage constant. SC has three modes: off, charging and discharging. When the stored energy becomes over the maximum limit or under the minimum limit, SC has to be turned off.

Figure 4 depicts the control scheme for SC converter. A configuration with outer voltage loop plus inner current loop is proposed. DC bus voltage  $V_{DC}$  is sensed, which is compared with the voltage reference  $V_{DCRef}$  and then the error  $\Delta V_{DC}$  is processed by a PI controller, which generates the SC current reference  $I_{SCRef}$ . The input to current loop is the difference between current reference  $I_{SCRef}$  and SC measured current  $I_{SC}$ . Additionally, the block “SC current limitation function” described by equation (4) is used to prevent SC overcharge and over discharge and to limit the current reference  $I_{SCRef}$  to the interval  $[I_{SCMin}, I_{SCMax}]$  (Thounthong *et al.*, 2009b):

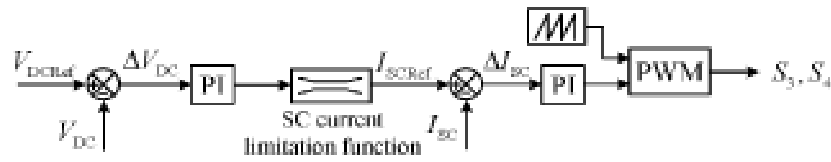


Fig. 4: Block diagram of the control scheme for SC

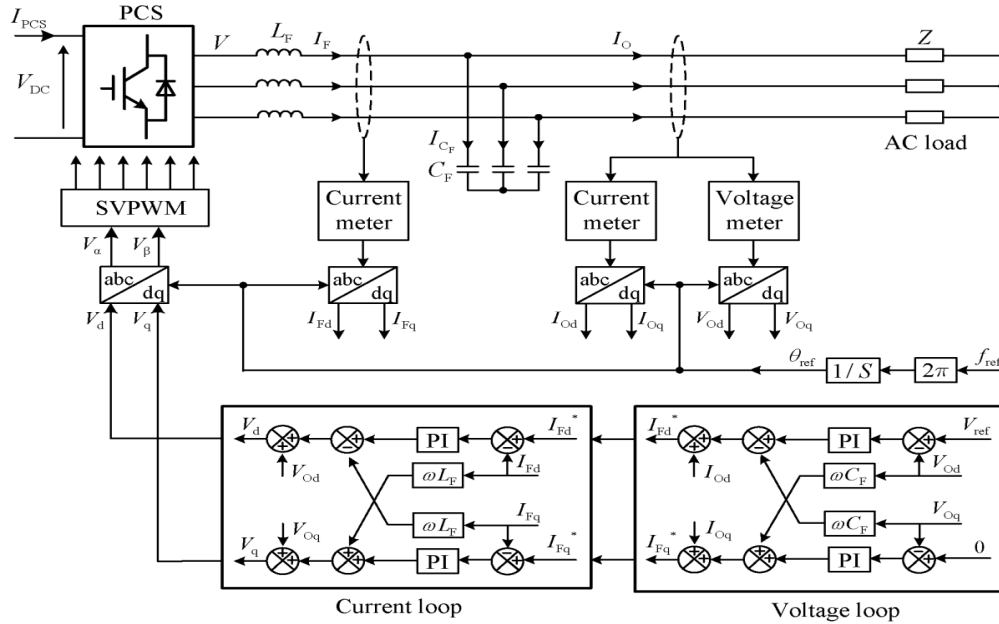


Fig. 5: Block diagram of the control scheme for PCS

$$\begin{cases} I_{SCMin} = -I_{SCRated} \cdot \min\left(1, \frac{V_{SCMax} - V_{SC}}{\Delta v}\right) \\ I_{SCMax} = I_{SCRated} \cdot \min\left(1, \frac{V_{SC} - V_{SCMin}}{\Delta v}\right) \end{cases} \quad (4)$$

where,

$I_{SCMin}$  : SC lowest

$I_{SCMax}$  : SC highest

$I_{SCRated}$  : SC rated current

$\Delta V$  : The regulation parameter

**Controller design for PCS:** In this hybrid system, PCS is a major part that can ensure constant voltage and frequency at PCC during variations in both load and solar insulation. Figure 5 shows the schematic diagram of the control strategy for PCS. It can be seen that the V/f controller consists of a fast internal current loop and an external voltage loop. The input of voltage loop is the desired voltage. In addition, for improving the performance of PI controller in dq control structure, cross-coupling terms and voltage feed-forward are also used (Yunwei *et al.*, 2004).

**Simulation analysis:** System simulation has been carried out using MATLAB/Simulink to verify the effectiveness of the proposed control scheme. The schematic diagram of the simulated HPS is provided, as shown in Fig. 6. It is difficult to say how the load, variable generation and energy storage system should be rated. In this study, it is assumed that the maximum load demand is equal to 30 kW and PV is also rated at 30 kW. To achieve uninterruptible power supply during cloudy day or at night, FC rated power is chosen to be 30 kW. A 40 kW PCS is used to supply ac load at PCC. The common dc bus voltage is set at 326 V. The switching frequencies of all converters are 20 kHz. The minimum and maximum accepted voltage values of SC are 150 and 300 V, respectively. SC initial voltage is set to be 250 V and its rated current is 400 A. In order to improve simulation speed and reflect control effect, the SC capacity, FC response speed, start threshold and stop threshold are set at 0.5 F, 1kA/s, 240 and 260 V, respectively. However, the parameters mentioned above should be set according to the technical data in practical applications.

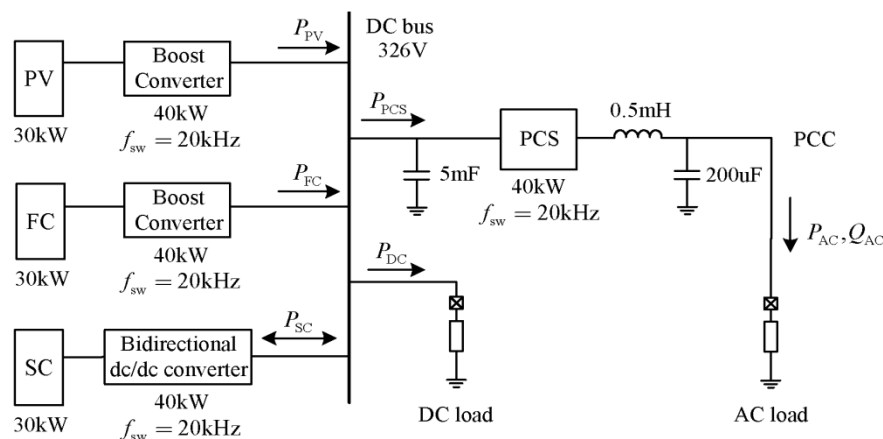


Fig. 6: Schematic diagram of the simulated system

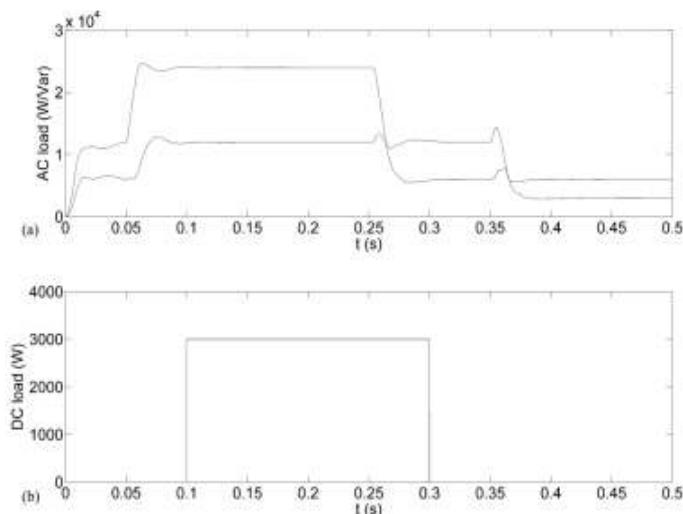


Fig. 7: Power demand of ac load and dc load

The load demand and solar radiation are time varied in terms of step. Figure 7 (a) shows the active and reactive power consumed by ac load and Fig. 7 (b) is the dc load demand. Solar radiation and PV output power are depicted in Fig. 8 (a) and (b), respectively. SC terminal voltage is shown in Fig. 9 (a) and FC output power is given in Fig. 9(b) and 10 shows the dc bus voltage. Figure 11 and 12 are the varieties of voltage and frequency at PCC, respectively. The detailed description of load-following capability of HPS is given next.

Initially, ac load is 12 kW+6 kVar, dc load is 0 kW; solar radiation is 600 W/m<sup>2</sup> and PV system generates approximately 10 kW. Because solar generation is less than load demand, the voltage across SC decreases due to its discharging; FC remains off until SC terminal voltage is less than 240 V. PCS starts and builds up V<sub>PCC</sub> starting from an initial voltage to

the nominal voltage. The value of V<sub>PCC</sub> under steady state reaches to 190 V and f<sub>PCC</sub> is held at 50 Hz.

At 0.05s, ac load is increased from 12 kW+6 kVar to 24 kW+12 kVar, dc load and solar generation remain at 0 and 10 kW. Due to a sudden increase in ac load, dc bus voltage drops and SC terminal voltage continues to decrease. The sharp increasing of load leads to a momentary fall in V<sub>PCC</sub> and f<sub>PCC</sub>, but V/f controller makes PCS supply the excessive power to maintain V<sub>PCC</sub> and f<sub>PCC</sub> stable.

At 0.1s, dc load is increased to 3kW. When V<sub>SC</sub> drops below 240 V, FC begin discharging and the output power is increased with a preset slope. For the sudden requirement of dc load, V<sub>DC</sub> goes down.

At 0.15s, solar radiation is raised to 800 W/m<sup>2</sup> and the value of P<sub>PV</sub> is raised to 20 kW. The illumination perturbation leads to a momentary rise in V<sub>DC</sub> due to the excessive active power. As generated power

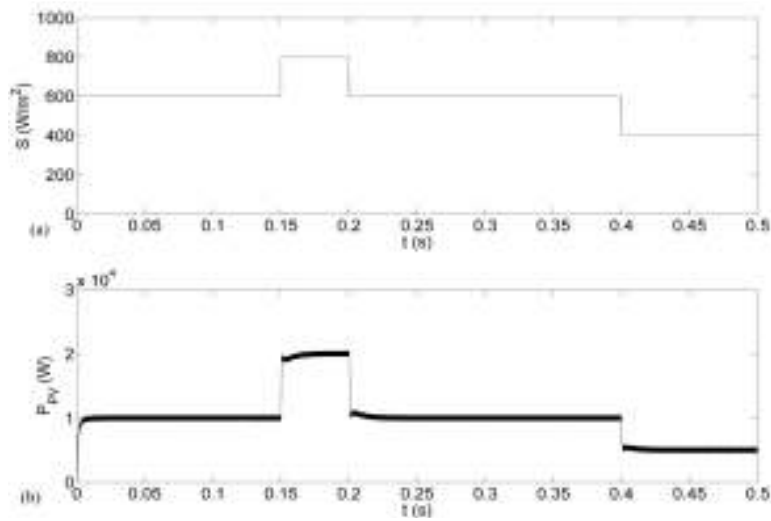


Fig. 8: Solar radiation and PV output power

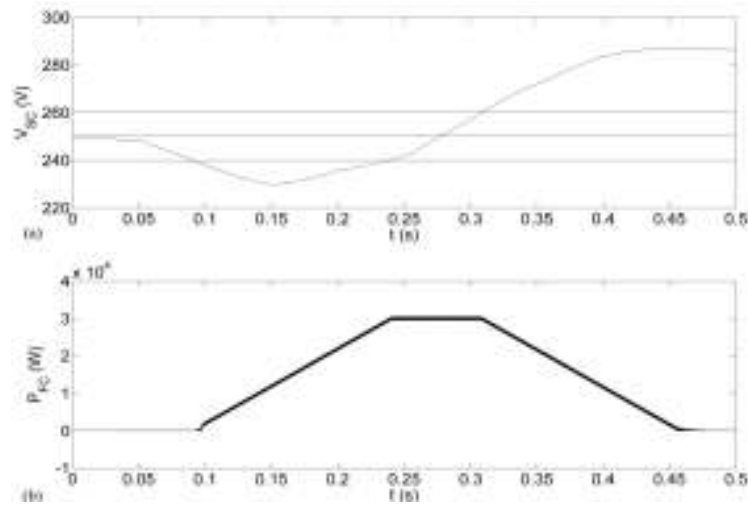


Fig. 9: SC terminal voltage and FC output power

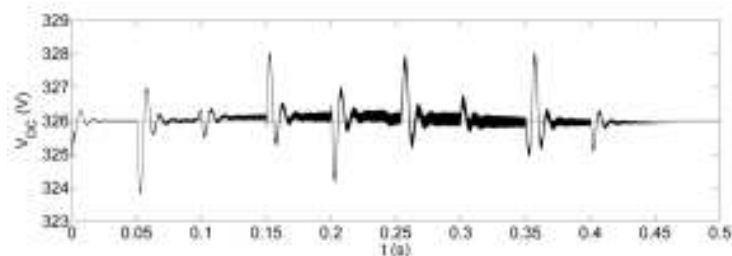


Fig. 10: DC bus voltage waveform

exceeds the load demand, SC is charged by surplus power with  $V_{SC}$  rising.

At 0.2s, solar radiation is reduced to  $600 \text{ W/m}^2$  and the illumination disturbance leads to a momentary fall

in  $V_{DC}$  due to the reduced  $P_{PV}$ . During the time period of  $t = 0.1\text{s}$  till  $t = 0.25\text{s}$ , there is no power variation at ac-link,  $V_{PCC}$  and  $f_{PCC}$  are well maintained within the acceptable range.

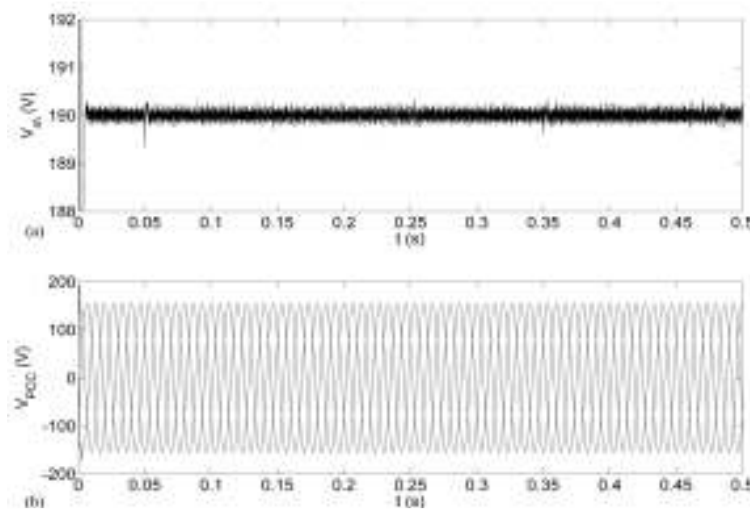


Fig. 11: Voltage variation at PCC

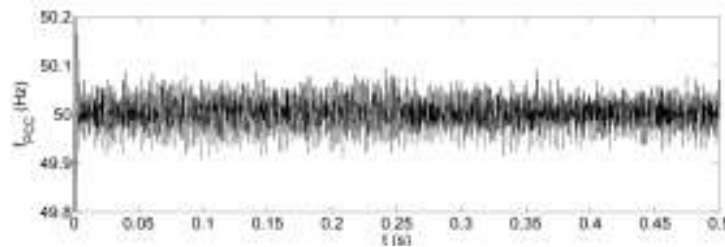


Fig. 12: Frequency variation at PCC

At 0.25s, ac load is decreased from 24 kW+12 k/V to 12 kW+6 k/V that results in the total imported power to PCC being significantly greater than ac load demand. Consequently,  $V_{PCC}$  and  $f_{PCC}$  try to go up, but for the voltage closed loop control of PCS,  $V_{PCC}$  and  $f_{PCC}$  decrease and hold at the desired level finally.

At 0.3s, dc load is removed from dc bus, that leads to a temporarily dc voltage rise. Since  $V_{SC}$  exceeds 260 V, FC returns back to standby state with a preset slope.

At 0.35s, ac load is reduced to 6kW+3kVar. At 0.4s, the solar radiation is reduced to 400 W/m<sup>2</sup> and the solar generated power is 5 kW.

From Fig. 10-12, it can be seen that dc voltage, ac voltage and frequency are kept constant under steady state; and the fluctuations vary in an acceptable range under the perturbations of solar radiation and load.

## CONCLUSION

The main study of this study is the hybridization of PV energy source with FC/SC system with appropriate power controllers to build an autonomous system. This HPS is mean to support critical load located in remote places where the utility grid is not available.

MPPT of PV is implemented to improve the system economics. Coordinated control strategy makes the system achieve 24 h power supply. Whenever the PV system cannot completely meet load demand, FC provides the power deficit; meanwhile the power slope is limited to avoid fuel starvation. SC plays an important role in stabilizing dc bus voltage and providing transient power. Also, V/f controller is designed to maintain the voltage and frequency at PCC within an acceptable range during the perturbations of solar radiation and load. Simulation studies have been conducted to show the system performance. The results demonstrate that the proposed control scheme not only improves the energy utilization, but also has the ability to track both dc and ac load changes.

## REFERENCES

- Ahmed, N.A., M. Miyatake and A.K. Al-Othman, 2008. Power fluctuations suppression of stand-alone hybrid generation combining solar photovoltaic/wind turbine and fuel cell systems. *Energ. Conver. Manage.*, 49(10): 2711-2719.

- Caisheng, W. and M.H. Nehrir, 2008. Power management of a stand-alone wind/ photovoltaic/ fuel cell energy system. *IEEE Trans. Energ. Convers.*, 23(3): 957-967.
- Chicco, G. and P. Mancarella, 2009. Distributed multi-generation: A comprehensive view. *Renewable Sustainable Energy Rev.*, 13(3): 535-551.
- Deshmukh, M.K. and S.S. Deshmukh, 2008. Modeling of hybrid renewable energy systems. *Renewable Sustainable Energy Rev.*, 12(1): 235-249.
- Esrām, T. and P.L. Chapman, 2007. Comparison of photovoltaic array maximum power point tracking techniques. *IEEE Trans. Energ. Convers.*, 22(2): 439-449.
- Jiayi, H., C.W. Jiang and R. Xu, 2008. A review on distributed energy resources and microgrid. *Renewable Sustainable Energy Rev.*, 12(9): 2472-2483.
- Kyoungsoo, R. and S. Rahman, 1998. Two-loop controller for maximizing performance of a grid-connected photovoltaic-fuel cell hybrid power plant. *IEEE Trans. Energ. Convers.*, 13(3): 276-281.
- Rahman, S. and K.S. Tam, 1988. A feasibility study of photovoltaic-fuel cell hybrid energy system. *IEEE Trans. Energy Convers.*, 3(1): 50-55.
- Reddy, K.N. and V. Agarwal, 2007. Utility-interactive hybrid distributed generation scheme with compensation feature. *IEEE Trans. Energ. Convers.*, 22(3): 666-673.
- Thounthong, P., B. Davat, S. Rael and P. Sethakul, 2009a. Fuel starvation. *IEEE Indus. Appl. Magazine*, 15(4): 52-59.
- Thounthong, P., S. Rael and B. Davat, 2009b. Analysis of supercapacitor as second source based on fuel cell power generation. *IEEE Trans. Energ. Convers.*, 24(1): 247-255.
- Thounthong, P., V. Chunkag, P. Sethakul, S. Sikkabut, S. Pierfederici and B. Davat, 2011. Energy management of fuel cell/solar cell/supercapacitor hybrid power source. *J. Power Sources*, 196(1): 313-324.
- Uzunoglu, M., O.C. Onar and M.S. Alam, 2009. Modeling, control and simulation of a PV/FC/UC based hybrid power generation system for stand-alone applications. *Renewable Energ.*, 34(3): 509-520.
- Yunwei, L., D.M. Vilathgamuwa and L. Poh Chiang, 2004. Design, analysis and real-time testing of a controller for multibus microgrid system. *IEEE Trans. Power Electr.*, 19(5): 1195-1204.